Efficient Fabrication and Enhanced Photocatalytic Activities of 3D-Ordered Films of Titania Hollow Spheres

Yuanzhi Li, Toyoki Kunitake,* and Shigenori Fujikawa

Frontier Research System (FRS), The Institute of Physical and Chemical Research (RIKEN), Hirosawa 2-1, Wako-shi, Saitama 351-0198, Japan

Received: March 30, 2006; In Final Form: May 16, 2006

Facile and effective approaches were developed to fabricate 3D-ordered films of titania hollow spheres with different sphere diameters. The shell thickness of the sphere was adjusted in the range of 20−40 nm by changing the casting cycle of the titania precursor. The photonic stop band was observed for the 3D-ordered film and was tunable by the sphere diameter and the shell thickness. The stop band shifted from 930 to 547 nm. Crystal violet dye adsorbed on the film exhibited more than two times higher absorbance than that on a reference film of a flat titania layer, probably due to the red edge effect of the stop band and/or to the multiple scattering effect. The enhanced absorbance led to more efficient photodegradation of the dye under visible light and under solar light irradiation. A maximum photocatalytic enhancement of 22% is achieved. Finally, the influence of TiO_2 morphology on photocatalytic activity was discussed. Compared with flat titania films, the existence of ordered macropores in titania spheres causes the stop band and a longer optical path due to multiple scattering. Both the red edge of the stop band and multiple scattering effects enhance the absorption of the dye, which results in the photocatalytic enhancement.

Introduction

In recent years, three-dimensionally (3D) ordered materials have attracted extensive interests for their possible applications in separation science, catalysis, and photonic materials such as optical filters, optical switches, waveguides, and low-threshold lasers.[1−4] As photonic materials, 3D-ordered titania films received special attention because of their unique properties, such as high refractive index, nonabsorption in the visible region, and high photocatalytic and photovoltaic efficiencies.[5−8] One of the most important applications of titania is photodetoxification of water and air pollutants. This has been a fast growing research area during recent decades.[9−11] Methods to increase their photocatalytic activity or to find new types of more efficient photocatalytic systems with visible or solar light currently remain an important issue.[12,13] Improvement of the photocatalytic activity by enhancing light harvesting efficiency has been quite limited.[14] It depends on strengthening of the interaction between titania and light, as affected by the morphology and macroscopic structure of titania. 3D-ordered titania with lattice spacings of the order of wavelengths of light exhibits a stop band in the region of visible light. Near the stop band edge, there exist low group velocities of light along with high electric-field intensity, which result in a strong interaction of light with titania or with dyes absorbed on titania.[15] On the other hand, multiple scattering in such 3D-ordered titania structures can improve greatly the light harvesting efficiency. Both the strong interactions between light and matter induced by the stop band edge effect and the multiple scattering effect will lead to enhanced photocatalytic activity.

Herein, we developed a facile and efficient approach for fabrication of 3D-ordered films of titania hollow spheres by using a 3D-ordered latex film as a template, investigated the stop band edge effect and the multiple scattering effect on photocatalytic activity, and provided a novel approach for designing efficient titania photocatalysts.

Experimental

Materials. Monodispersed polystyrene spheres with different diameters were bought from Polysciences: latex A (2.62% solid latex, diameter 202 nm, standard deviation 10 nm), latex B (2.70% solid latex, diameter 356 nm, standard deviation 14 nm), and latex C (2.71% solid latex, diameter 548 nm, standard deviation 16 nm). Glass slides were products from Iwaki Glass, Japan. Reagent quality sulfuric acid (95%), hydrogen peroxide (30%), titanium (IV) butoxide, and hydrochloric acid (37%) were bought from Wako Pure Chem., Japan.

Fabrication of Ordered Latex Films. Glass slides (1.9 cm × 1.3 cm) used for the experiment were first treated with a mixture of 30% hydrogen peroxide and 70% sulfuric acid for 8 h, washed with deionized water, and finally dried by flushing with nitrogen gas. 3D-ordered latex films were fabricated by our newly developed sonication-assisted casting.[16] The fabrication procedure is as follows. The glass slide was placed on the bottom of a beaker. The beaker was placed in water in an ultrasonic apparatus (Yamato 1510). Thirty μL of latex dispersions was dropped on the glass slide and spread uniformly on the whole area of the slide with the tip of a pipet, and then, the ultrasonic apparatus was turned on. The water was allowed to evaporate at ambient temperature under sonication, and 3D-ordered latex films were formed on the glass slide.

Fabrication of 3D-Ordered Hollow-Sphere Films of TiO_2. Since the template latices in the film are connected with each other only via van der Waals contacts, they are prone to disintegrate and fall off from glass slides into solution during immersion for matrix penetration. To avoid this problem, we employed a gas-phase surface sol−gel process (G-SSG) to make

* Tel.: +81-48-467-9601. Fax: +81-48-464-6391. E-mail: kunitake@ruby.ocn.ne.jp.

10.1021/jp061979z CCC: $33.50
Published on Web 06/14/2006

the latex film robust.[16] Two mL of neat titanium (IV) butoxide was placed in a small glass bottle (Φ2.7 × 5.5 cm) in a temperature-controlled heater. The bottle was saturated with titanium (IV) butoxide vapor by heating at 70 °C for 20 min. Then, latex films on glass slides (1.9 cm × 1.3 cm) were placed in this atmosphere for 3 min and transferred to an oven with 70% humidity and 40 °C for 3 min to hydrolyze the adsorbed titanium (IV) butoxide and to generate a reactive titania surface. This process was repeated 3 times.

Subsequent titania casting was conducted as follows. Hydrochloric acid (25 μL, 1.5 mol/L) and 50 μL of deionized water were mixed with 5 mL of ethanol, and then, 25 μL of neat titanium (IV) butoxide was added under magnetic stirring. Fifty μL of the mixture was spread uniformly on the whole area of the 3D-ordered latex film and was allowed to penetrate into the film interior. After the solvent was evaporated, the film was dried at ambient temperature and transferred to an oven with controlled humidity (70%) and temperature (50 °C) for 5 min. The adsorbed titania precursor was completely hydrolyzed to amorphous titania. The penetration process was repeated 10 times. The film was covered by another glass slide and placed in 0.08 mol/L dilute hydrochloric acid in a small bottle. The bottle was kept in a container at 70 °C for 48 h. The amorphous titania was transformed to anatase in the liquid−solid reaction.[17] To remove the organic latex, the sample was heated to 480 °C from room temperature at a rate of 1 °C/min and kept at the temperature for 1 h. A reference titania thin film without the photonic crystal structure was prepared on a glass slide by a similar procedure. The reference titania thin film contained same amount of titania (0.196 g) as the titania films of hollow spheres. The thickness of the reference titania thin film is 1.4 μm.

Scanning electron microscopy (SEM) images were obtained by using a Hitachi S-5200 scanning electron microscope. X-ray diffraction (XRD) patterns were obtained on a Rigaku Dmax X-ray diffractometer using Cu Kα radiation. Absorption spectra were recorded on a UV3100 UV−vis-NIR spectrophotometer. For UV measurement, 20 μL of 5.0×10^{-4} mol/L crystal violet in ethanol was dropped on the hollow titania film. After evaporation of ethanol at room temperature in the dark, absorption spectra of the dye was obtained by subtracting the absorption of the titania film as background.

Photocatalytic Activity. The photodegradation of crystal violet was chosen to evaluate the photocatalytic activity of the titania sample. First, 20 μL of 1.0 mmol/L crystal violet in ethanol was dropped on the film. After drying at room temperature in the dark, the film was fixed on a shelf under AM 1.5 solar light and the solar light was turned on. A UV cut-filter (L42), which can filter out UV light with wavelengths below 420 nm, was placed between the film and solar light. After irradiation, the film was immersed in 6 mL of ethanol to dissolve the unreacted dye and was washed with 1 mL of ethanol. The dye concentration was determined by measuring the UV−vis absorbance of the washing.

Results and discussion

Fabrication of TiO_2 Hollow-Sphere Film. There have been a number of reports on fabrication of 3D-ordered titania layers, often as inverse opal.[5−7] Only limited reports are related to the fabrication of titania hollow spheres.[8] In the latter preparation, it is necessary for titania precursor to penetrate into pores among the ordered latex and to be uniformly adsorbed on the latex surface alone. An inverse opal would result if the titania precursor filled the pores completely. To avoid this situation, we used a gas-phase surface sol−gel process to form reactive titania layers on the latex surface.[16] Titanium (IV) butoxide is readily hydrolyzed by ambient moisture to give titania precipitates. This would block the pore of the top surface of the ordered latex and prevent the titania precursor from further penetration into the inner pore. In our experiment, quick hydrolysis and precipitation of titanium (IV) butoxide were avoided by adding dilute hydrochloric acid to titanium (IV) butoxide in ethanol. The resulting transparent precursor solution remained stable without precipitation for 1 week.

The starting 3D-ordered latex film prior to titania casting has been shown to possess line dislocations.[16] Calcination led to 7.9% shrinkage of the titania film along line dislocations. Complete removal of the organic moiety upon calcination was confirmed by Fourier transform infrared (FTIR) spectroscopy. Strong C−H stretching bands in the range of 2850−3080 cm^{-1} (ref 18) that were observed before calcination for the latex film completely disappeared upon calcination.

Figure 1 shows SEM images of a film of hollow titania spheres. The top surface given in Figure 1a is composed of a closely packed, hexagonal array of hollow titania spheres with a diameter of 328 nm. The cross-section SEM image of Figure 1b exhibits 16 layers of titania spheres closely packed along the direction perpendicular to the surface. Figure 1c presents a higher-magnification SEM image of intentionally broken titania spheres that shows a smooth inner surface and a relatively rough outer surface. The hollow spheres are connected to their neighbors through pores. The titania shell has a uniform thickness of 37 nm. Since the titania casting was repeated 10 times, the individual casting leads to a thickness increment of 3.7 nm. This casting method is reproducible, facile, and efficient, and we can readily fabricate large-scale 3D-ordered films of titania hollow spheres. Furthermore, we can readily adjust the shell thickness of the hollow spheres just by changing the casting cycles of the titania precursor. When the casting cycle is decreased from 10 to 7, the film top morphology and the diameter of the hollow sphere essentially remained unchanged but the shell thickness decreased from 37 to 26 nm (Figure 1c and d).

Figure 2 shows an XRD pattern of the 3D-ordered film of titania hollow spheres (diameter 328 nm, shell thickness 26 nm). There are observed four weak diffraction peaks characteristic of anatase titania in the amorphous background of the glass.

The current approach was similarly applied to fabrication of 3D-ordered films of titania hollow spheres with different sizes. Figure 3a and b shows SEM images of the film surface as closely packed, hexagonal arrays of titania spheres. The corresponding cross-section SEM images exhibit vertical ordering of the titania spheres. Intentionally broken titania spheres with diameters of 198 and 496 nm (Figures 3c and d) show hollow structures with shell thicknesses of 35 and 20 nm, respectively.

UV−vis-NIR Spectroscopy. We examined spectroscopic properties of the 3D-ordered films of titania hollow spheres with a UV−vis-NIR spectrophotometer. The incident light was perpendicular to the film plane. Figure 4A shows absorption spectra of the titania film. Because a 3D-ordered film of titania can strongly diffract light of a specific wavelength, there exists a stop band that excludes the passage of photons of a chosen range of frequencies. For the sphere diameter of 496 nm, there is observed a photonic stop band at 930 nm. With a decrease in the diameter to 328 nm, the stop band shifts to 555 nm. A further decrease of the diameter to 198 nm causes overlapping of the stop band with the intrinsic absorption of titania. For the case of the sphere diameter of 328 nm, the stop band is slightly

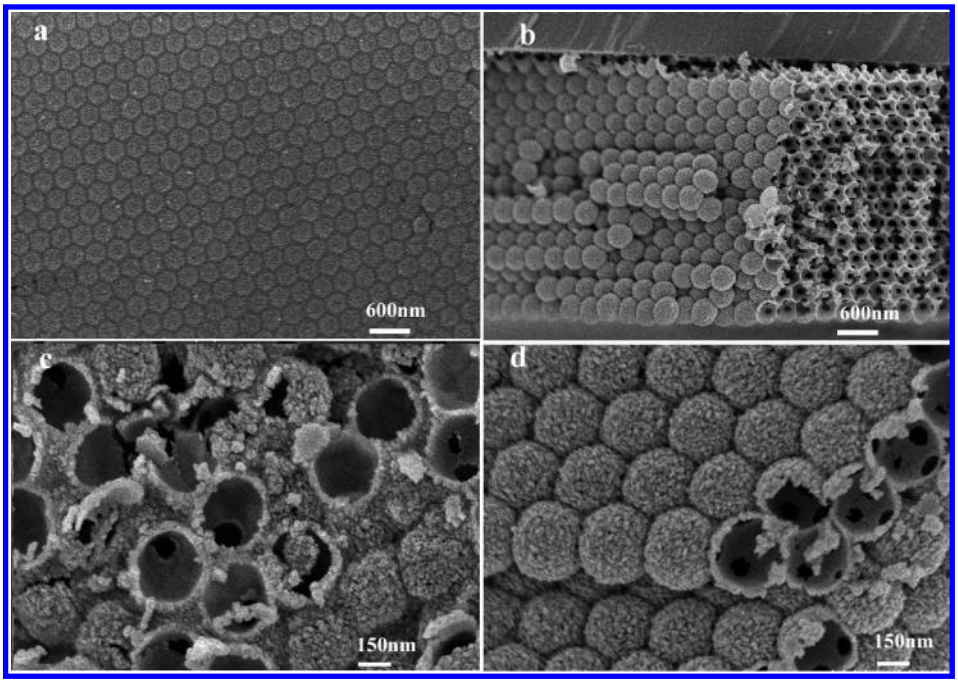

Figure 1. SEM images of the 3D-ordered titania films of hollow spheres (diameter 328 nm): (a) top morphology; (b) cross-section view; (c and d) intentionally broken spheres with different thicknesses of (c) 37 and (d) 26 nm.

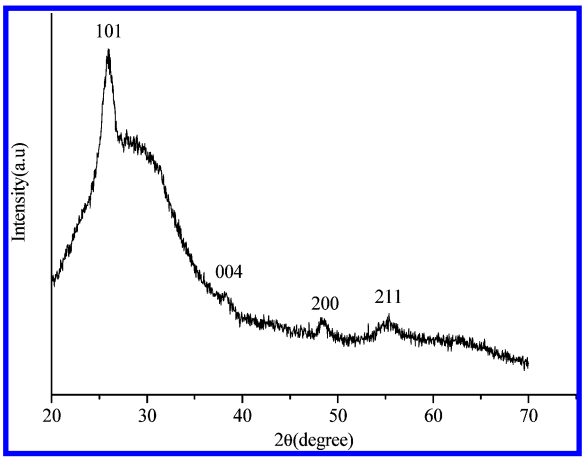

Figure 2. XRD pattern of the 3D-ordered film of titania hollow spheres (diameter 328 nm, shell thickness 26 nm).

shifted from 555 to 547 nm by changing the shell thickness from 37 to 26 nm.

Figure 4B shows absorption spectra of the dye adsorbed on the titania films. The dye adsorbed on the reference (flat) titania film is characterized by one absorption peak at $\lambda_{max} = 592$ nm with a shoulder peak at $\lambda_{min} = 535$ nm. The molar extinction coefficient (ϵ) at λ_{max} is 3.5×10^4 $M^{-1}\cdot cm^{-1}$. In contrast, the dye adsorbed onto an ordered film of hollow titania spheres (diameter 328 nm, shell thickness 26 nm) shows a strong enhancement of absorbance at the red edge of the stop band. The molar extinction coefficient (8.2×10^4 $M^{-1}\cdot cm^{-1}$) at λ_{max} becomes more than two times larger. This phenomenon is attributed the strong interaction of light with absorber on titania, since there exist low group velocities of light along with high electric-field intensity near the red edge of the stop band.[15] The same effect was observed when the stop band was tuned from 547 to 555 nm by increasing the shell thickness from 26 to 37 nm. The maximum molar extinction coefficient at λ_{max} (ϵ_{max}) of the dye on the titania sphere (diameter 328 nm, shell thickness 37 nm) is 7.6×10^4 $M^{-1}\cdot cm^{-1}$. When there is no spectral overlap with the stop band (for the case of the hollow sphere diameters of 198 and 496 nm), the spectral shape of the dye is similar to that of the dye adsorbed on the reference titania film, as shown in Figure 4B. However, the corresponding absorption intensity is enhanced relative to that of the latter film. The ϵ_{max} of the dye adsorbed on these titania hollow spheres with diameters of 198 and 496 nm is 5.3×10^4 and 6.8×10^4 $M^{-1}\cdot cm^{-1}$, respectively.

It is known that the optical path in a thin film becomes longer due to multiple scattering, when light wavelength is comparable to the periodicity of the photonic crystal.[19] The longer optical path in the titania sphere film causes an enhancement of optical absorption, resulting in a greater light harvesting efficiency. This effect is more pronounced in the case of the titania sphere with a diameter of 496 nm than that with a diameter of 198 nm, because the former film has a periodicity closer to the absorption wavelength of the dye ($\lambda_{max} = 592$ nm) than that of the latter.

These results show that there exist two favorable effects—multiple scattering and the red edge effect of the stop band—for absorbance enhancement, when dyes are adsorbed on 3D-ordered films of titania.

Photocatalytic Activity. Effective utilization of solar light to degrade organic wastes and spent dyes in the presence of titania is expected to provide an attractive approach for environmental remediation.[20] We chose photodegradation of crystal violet dye with visible light and solar light to evaluate the photocatalytic activity of the ordered titania sphere. Figure 5A shows the time course of the decrease in the dye concentration with irradiation of the visible light. Although crystal violet adsorbed on a glass slide is slowly photodegraded with time, the flat titania film (reference film) clearly accelerates the photodegradation process (curve a). Among the titania sphere films, the titania sphere with a 328 nm diameter and 26 nm shell gives the highest efficiency (curve e). The reference titania film and the titania sphere films were prepared under same procedure and experimental conditions, which result in their similar physicochemical properties, such as crystalline structure (anatase), crystal size, surface state, etc. The only difference among the films is the existence of 3D-ordered macropores in the titania sphere films, which does not result in an obvious

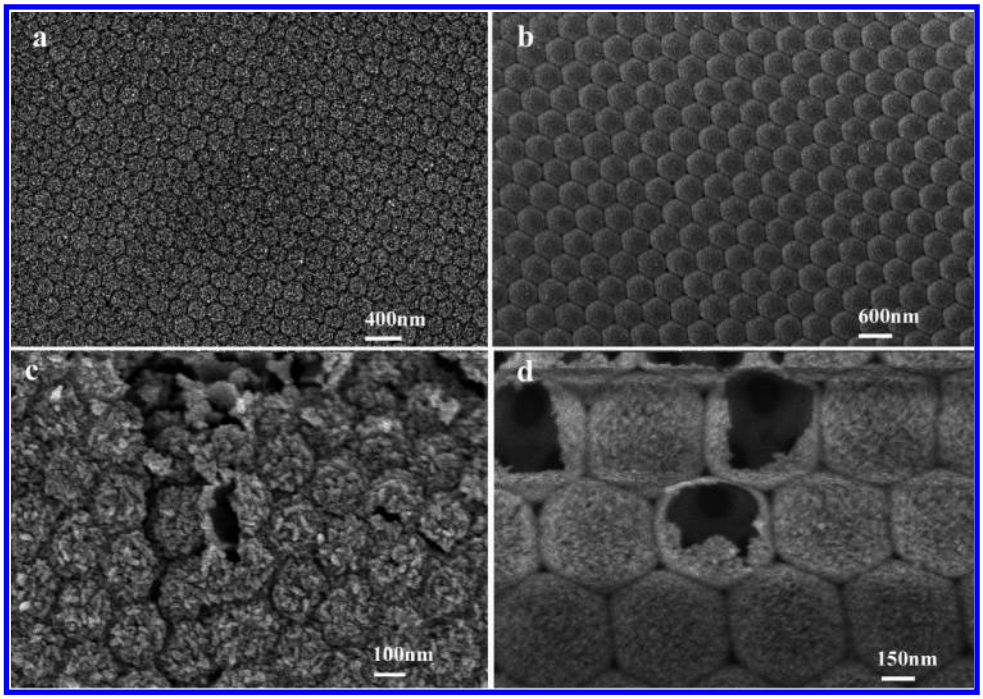

Figure 3. SEM images of 3D-ordered films of titania hollow spheres. The top morphology is shown for the following: (a) sphere diameter of 198 nm; (b) sphere diameter of 496 nm. Intentionally broken spheres of (c) 198 and (d) 496 nm diameters are shown.

increase of the specific surface area. Therefore, the higher photocatlytic activity of the titania sphere films than the reference titania film could not be explained by their difference of physicochemical properties and surface area. Dye photodegradation under visible illumination proceeds according to the following mechanism.[13,21] Dyes, rather than catalysts, are excited by visible light to the appropriate singlet and triplet states through intersystem crossing, followed by electron injection into the titania conduction band. The injected electrons, TiO_2 (e^-), reduce surface chemisorbed oxidants, typically O_2, to yield oxidizing species such as superoxide radical anions O_2^- and subsequently $^{\bullet}OH$ radicals that cause the degradation of dyes. As can be seen from Figure 4, the dye absorbed on the titania hollow sphere (diameter 328 nm, shell thickness 26 nm) shows an absorbance enhancement due to the red edge effect of the stop band, as compared with the one on the reference titania film. This leads to enhancement of the photoconversion efficiency[15a] and, finally, to the improvement of photocatalytic activity. This photocatalytic enhancement is sensitive to the separation of the maximum dye absorption relative to the minimum of the stop band. When the separation decreases, the photocatalytic activity decreases (Figure 5A lines d and e).

The stop band of the titania hollow sphere (diameter 496 nm) is outside of both the visible range of solar light and the dye absorption region, and its photocatalytic activity could be similar to that of the reference titania film. However, a somewhat higher photocatalytic actitivity was observed in Figure 5A, curve c. This difference may be caused by the multiple scattering effect, as discussed above. In contrast, the hollow sphere film (diameter 198 nm) has a photocatalytic activity (curve b) similar to that of the reference titania thin film. The multiple scattering effect may be negligible in the latter case, since the light wavelength and the size of the hollow sphere is much different.

Figure 5B demonstrates the time course of the dye degradation with irradiation of AM 1.5 solar light which contains a small portion of UV light (shorter than 420 nm). The dye degradation becomes more efficient, when compared with the visible light data. In the case of the reference titania film, the enhancement is approximately 10%. While the photocatalytic

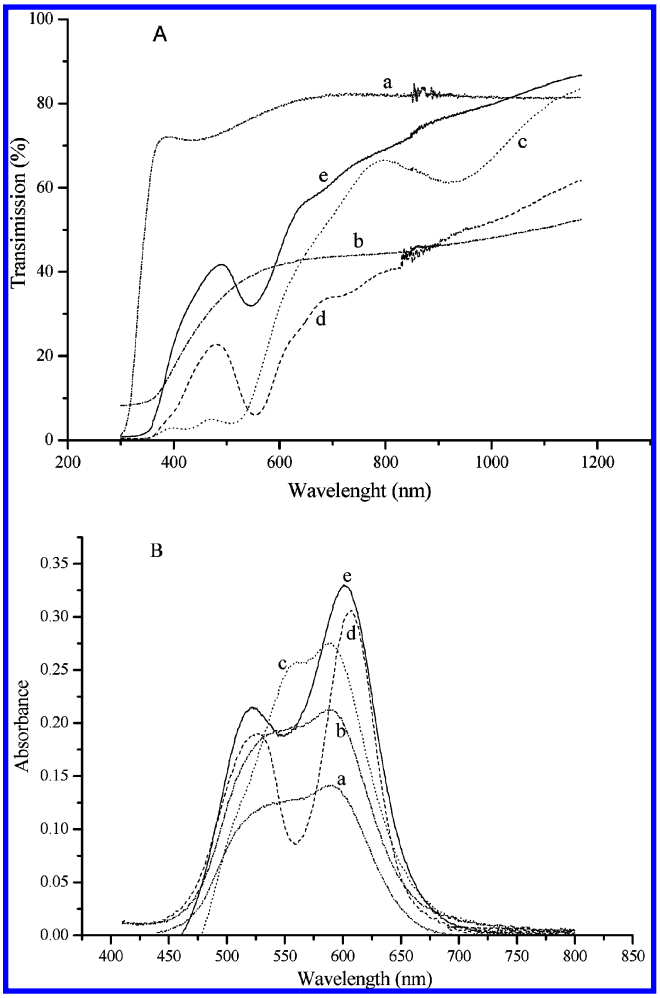

Figure 4. (A) Transmission spectra of the 3D-ordered films of titania hollow spheres: (a) reference titania flat film, (b) diameter 198 nm, (c) diameter 496 nm, (d) diameter 328 nm (shell thickness 37 nm), (e) diameter 328 nm (shell thickness 26 nm). (B) Absorption spectra of crystal violet as adsorbed on titania hollow spheres.

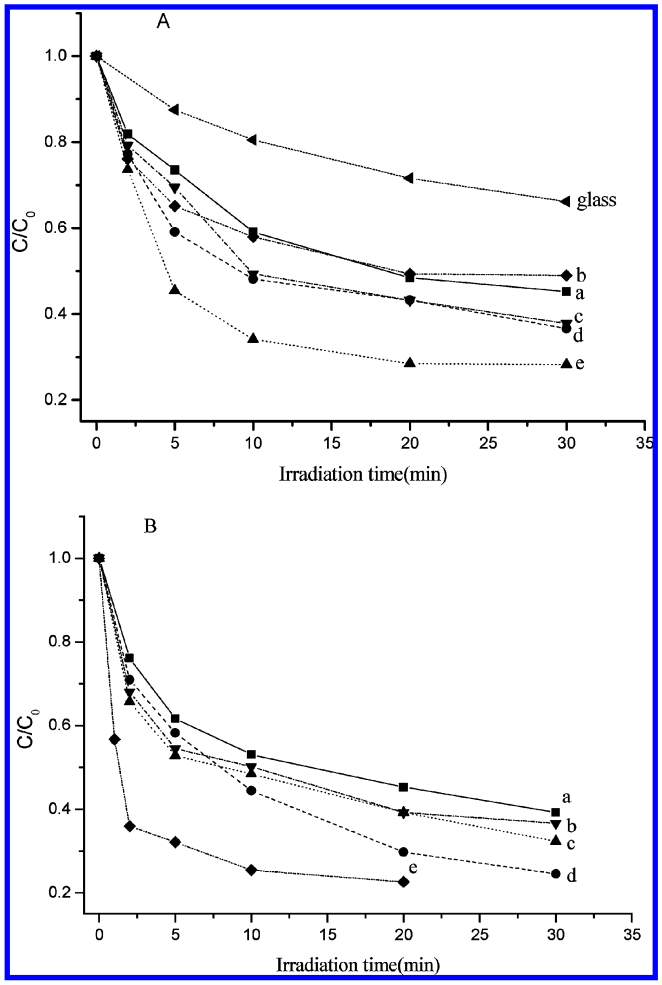

Figure 5. Decreases in the dye concentration upon irradiation with (A) visible light and (B) solar light. Crystal violet dye is adsorbed on (a) reference titania flat film and on the films of titania hollow spheres with different sphere diameters and shell thicknesses: (b) diameter 198 nm, (c) diameter 496 nm, (d) diameter 328 nm (shell thickness 37 nm), (e) diameter 328 nm (shell thickness 26 nm).

activity of the titania spheres (diameter 328 nm, shell thickness 37 nm) is close to the titania spheres of diameter 498 nm under visible light irradiation, the former film exhibits higher photocatalytic activity than the latter under solar light irradiation. This is attributed to the more pronounced multiple scattering of UV light in the former films than in the latter. The former films have a periodicity closer to the UV wavelength involved in solar light. These results further confirm the above supposition that the enhanced photocatalytic activity is derived from multiple scattering effects. An especially high photocatalytic activity (curve e) was found in the case of the titania spheres with a diameter of 328 nm and shell thickness of 26 nm, probably due to the synergy of the red edge effect of the stop band and the multiple scattering effect.

Conclusion

In summary, we demonstrated that the photocatalytic activity of ordered titania hollow spheres is enhanced most probably by the stop band effect and multiple scattering. The influence of the titania morphology on the light harvesting efficiency has been discussed intensively in recent years. The inverse-opal photonic crystal fabricated via ordered latex films as template was studied most frequently for this purpose,[15] indicating the presence of the above two effects. At the same time, Wang et al. reported the importance of macrochannels in titania that increase photoabsorption efficiency and allow efficient diffusion of gaseous molecules.[14] Our results indicate that the hollow sphere morphology is convenient for creating some of these effects. Organic, inorganic, and metallic modifications of hollow spheres can be done quite readily. Further combination of material function and photonic properties would be useful for development of novel functional systems.

References and Notes

(1) Park, S. H.; Xia, Y. *Langmuir* **1999**, *15*, 266−273.

(2) Tran, P. *J. Opt. Soc. Am. B* **1997**, *14*, 2589−2595.

(3) Vogelaar, L.; Nijda, W.; van Wolferen, H. A. G. M.; de Ridder, R. M.; Segerink, F. B.; Kuipers, E. F. L.; van Hulst, N. F. *Adv. Mater.* **2001**, *13*, 1551.

(4) Lopez, C. *Adv. Mater.* **2003**, *15*, 1679.

(5) (a) Holland, B. T.; Blanford, C. F.; Stein, A. *Science* **1998**, *281*, 538. (b) Wijnhoven, J. E. G. J.; Bechger, L.; Vos, W. L. *Chem. Mater.* **2001**, *13*, 4486. (c) Turner, M. E.; Trentler, T. J.; Colvin, V. L. *Adv. Mater.* **2001**, *13*, 180. (d) Yi, G. R.; Moon, J. H.; Yang, S. M. *Chem. Mater.* **2001**, *13*, 2613. (e) Schroden, R. C.; Al-Daous, M.; Blanford, C. F.; Stein, A. *Chem. Mater.* **2002**, *14*, 3305. (f) Dong, W. T.; Bongard, H. J.; Marlow, F. *Chem. Mater.* **2003**, *15*, 568.

(6) King, J. S.; Graugnard, E.; Summers, C. J. *Adv. Mater.* **2005**, *17*, 1010.

(7) Manoharan, V. N.; Imhof, A.; Thorne, J. D.; Pine, D. J. *Adv. Mater.* **2001**, *13*, 447.

(8) (a) Zhong, Z. Y.; Yin, Y. D.; Gates, B.; Xia, Y. *Adv. Mater.* **2000**, *12*, 206. (b) Jiang, P.; Bertone, J. F.; Volvin, V. L. *Science*, **2001**, *291*, 453.

(9) Fujishima, A.; Rao, T. N.; Tryk, D. A. *J. Photochem. Photobiol., C* **2000**, *1*, 1.

(10) Linsebigler, A. L.; Lu, G.; T. Yates, J. J. *Chem. Rev.* **1995**, *95*, 735.

(11) Legrini, O.; Oliveros, E.; Braun, A. M. *Chem. Rev.* **1993**, *93*, 671.

(12) Stathatos, E.; Petrova, T.; Lianos, P. *Langmuir* **2001**, *17*, 5025.

(13) Zhao, W.; Chen, C. C.; Li, X. Z.; Zhao, J. C. *J. Phys. Chem. B.* **2002**, *106*, 5022.

(14) Wang, X. C.; Yu, J. C.; Ho, C. M.; Hou, Y. D.; Fu, X. Z. *Langmuir* **2005**, *21*, 2552.

(15) (a) Nishimura, S.; Abrams, N.; Lewis, B. A.; Halaoui, L. I.; Mallouk, T. E.; Benkstein, K. D.; van de Lagemaat, J.; Frank, A. J. *J. Am. Chem. Soc.* **2003**, *125*, 6306. (b) Halaoui, L. I.; Abraams, N. M.; Mallouk, T. E. *J. Phys. Chem. B.* **2005**, *109*, 6334.

(16) Li, Y. Z.; Kunitake, T.; Fujikawa, S. *Colloids Surf. A* **2006**, *275* (1−3), 209−217.

(17) Li, Y. Z.; Lee, N. H.; Hwang, D. S.; Song, J. S.; Lee, E. G.; Kim, S. J. *Langmuir* **2004**, *20*, 10838.

(18) Dean, J. A. *LANGE'S Handbook of Chemistry*; McGraw-Hill: New York, 1999.

(19) Usami, A.; Ozaki, H. *J. Phys. Chem. B.* **2005**, *109*, 2591.

(20) Nasr, C. H.; Vinodgopal, K.; Fisher, L.; Hotchandani, S.; Chstto-padhyay, A. K.; Kamat, P. V. *J. Phys. Chem. B.* **1996**, *100*, 8436.

(21) (a) Vinodgopal, K.; Wynkoop, D. E.; Kamat, P. V. *Environ. Sci. Technol.* **1996**, *30*, 1660. (b) Vinodgopal, K.; Kamat, P. V. *Environ. Sci. Technol.* **1995**, *29*, 841.